

# Size and doping effects on the coercive field of ferroelectric nanoparticles

Th. Michael, S. Trimper

*Institut für Physik, Martin-Luther-Universität, D-06099 Halle Germany\**

J. M. Wesselinowa

*University of Sofia, Department of Physics*

*Blvd. J. Bouchier 5, 1164 Sofia, Bulgaria<sup>†</sup>*

(Dated: May 1, 2019)

## Abstract

A microscopic model for describing ferroelectric nanoparticles is proposed which allows us to calculate the polarization as a function of an external electric field, the temperature, the defect concentration and the particle size. The interaction of the constituents of the material, arranged in layers, depends on both the coupling strength at the surface and that of defect shells in addition to the bulk values. The analysis is based on an Ising model in a transverse field, modified in such a manner to study the influence of size and doping effects on the hysteresis loop of the nanoparticles. Using a Green's function technique in real space we find the coercive field, the remanent polarization and the critical temperature which differ significantly from the bulk behavior. Depending on the varying coupling strength due to the kind of doping ions and the surface configuration, the coercive field and the remanent polarization can either increase or decrease in comparison to the bulk behavior. The theoretical results are compared with a variety of different experimental data.

PACS numbers: 77.80.-e, 77.80.Dj, 77.80.Bh, 68.55.Ln

---

\*Electronic address: thomas.michael@physik.uni-halle.de; steffen.trimper@physik.uni-halle.de

<sup>†</sup>Electronic address: julia@phys.uni-sofia.bg

## I. INTRODUCTION

The interesting physical properties and the ability to store information via a switchable polarization have moved ferroelectric materials into the focus of research. One important application, the non-volatile memories with ferroelectric capacitor materials are known as ferroelectric random access memories (FRAM). The processing issues involved in the high density integration process are highly dependent on the ferroelectric and electrode-barrier materials. Hence, the selection of materials is a decisive factor in determining the performance of the device [1]. In view of fundamental ferroelectric properties, there are two potential ferroelectric materials for FRAM applications, namely  $\text{Pb}(\text{Zr,Ti})\text{TiO}_3$  (PZT) and  $\text{SrBi}_2\text{Ta}_2\text{O}_9$  (SBT) [2]. They possess a high remanent polarization  $\sigma_r$ , low coercive electric field  $E_c$ , which characterizes the polarization reversal, and low dielectric loss. The use of ferroelectric thin films and small particles in high density non-volatile random access memories is based on the ability of ferroelectrics being positioned in two opposite polarization states by an external electric field [3]. It is therefore of great interest to study the thickness dependence of  $E_c$  for small ferroelectric (FE) particles. This coercive electric field usually increases significantly with decreasing film thickness or particle size [4, 5, 6, 7]. The strength of the coercive field is related to the ease of domain nucleation and domain-wall motion, while the permittivity is related to the density of domain walls and their mobility at low fields. A diversity of different explanations have been proposed in the past for this size effect, including the surface pinning of domain walls and the influence of an internal electric field on the domain nucleation in depleted films. Current observations state that the thickness dependence of the coercive field in PZT films with metallic electrodes is caused mainly by the presence of a non-ferroelectric layer at the film/electrode interface. A parabolic-like relationship between the coercive field and grain size of ferroelectric PZT films is obtained by Liu et al. [8]. Nevertheless, the curvature of the parabolic curves varies with the thickness. It is demonstrated that the curvature increases as the thickness of the film decreases. The influence of thickness on the curvature was explained by the dielectric dependence on the thickness. The coercive field of a FE particle is stress sensitive. Lebedev and Akedo [9] have shown that the increase of internal compressive stress for thinner PZT films led to the increase of the coercive field and breakdown electrical strength, while tensile stress decreases  $\sigma_r$  and  $E_c$ .

In order to obtain high remanent polarization and low coercive field there are many experiments with doped ferroelectric thin films and small particles. By adding oxide group softeners, hardeners and stabilizers one can modify these materials. Softeners (donors) reduce the coercive field strength and the elastic modulus and increase the permittivity, the dielectric constant and the mechanical losses. Doping of hardeners (acceptors) gives higher conductivity, reduces the dielectric constant and increases the mechanical quality factor [10]. Multiple ion occupation of A and/or B sites in  $ABO_3$  compounds can affect the lattice parameters and the tetragonal distortion ( $c/a$ ). As a consequence a change of the physical properties as the polarization and the phase transition temperature is expected. Direct evidence of A-site-deficient SBT and its enhanced ferroelectric characteristics is given by Noguchi et al. [11]. The increase of Ba concentration in PLZT ceramics done by Ramam [15] and the substitution of La in PZT nanopowders and thin films lead to a marked decrease in  $T_c$ ,  $\sigma_r$  and  $E_c$  [12, 13, 14]. An enhancement of dielectric constant and lower  $T_c$  and  $E_c$  were observed by addition of PT particles to a PZT matrix [16].

There is only a small number of theoretical studies of the dependence of the coercive field in ferroelectric small particles. Lo [17] has investigated theoretically the thickness effect in ferroelectric thin films using Landau-Khalatnikov theory. Ferroelectric properties such as the hysteresis loop, and its associated coercive field and the remanent polarization of various film thickness have been numerically simulated. Recently FE thin films has been studied in dependence on the film thickness, where the phenomenological Landau theory is applied [18]. The authors stress that the thickness-dependent coercive field represents the intrinsic coercive field. Moreover, they point out to the role of defects observed in real ferroelectric thin films. In general the number of defects increases with the film thickness.

The aim of the present paper is to study the size dependence and doping effects of ferroelectric small particles using a more refined model, in which the microscopic interaction between the constituent parts of the material are explicitly taken into account. A adequate candidate is the Ising model in a transverse field (TIM), where ferroelectric properties are described by pseudo-spin operators. The model is quite successful for bulk material [19, 20]. Here we extend the applicability of the model to nanoparticles. We utilize a Green's function technique to investigate the interacting system, which has to be formulated in real space because of the lack of translational invariance.

## II. THE MODEL AND THE GREEN'S FUNCTION

Following Blinc and Žekš [19] the FE constituents are described by pseudo-spin operators. We consider a spherical particle characterized by fixing the origin at a certain spin in the center of the particle. All other spins within the particle are ordered in shells, which are numbered by  $n = 0, 1, \dots, N$ . Here  $n = 0$  denotes the central spin and  $n = N$  represents the surface of the system, see Fig. 1.

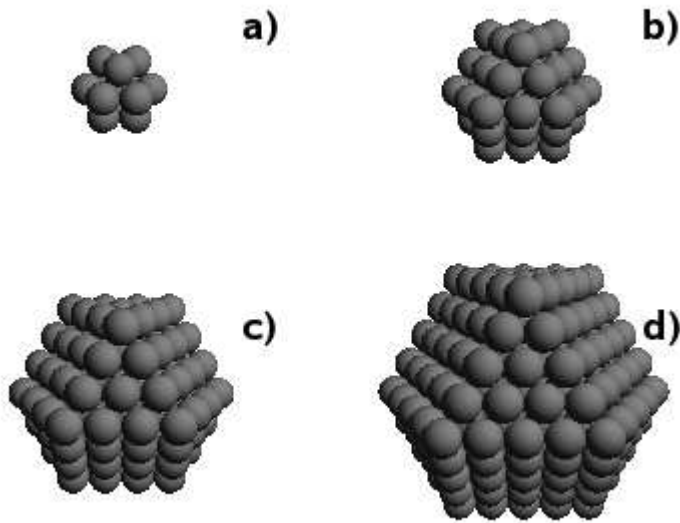


FIG. 1: Array of the ferroelectric nanoparticles composed of different shells. Each sphere represents a spin situated in the center, where (a) consists of one central spin plus  $N = 1$  shell, (b)  $N = 2$ , (c)  $N = 3$ , (d)  $N = 4$ .

The surface effects are included by different coupling parameters within the surface shell and within the bulk.

The Hamiltonian of the TIM includes both, bulk and surface properties. It reads

$$H = -\frac{1}{2} \sum_{ij} J_{ij} S_i^z S_j^z - \sum_i \Omega_i S_i^x - \mu E \sum_i S_i^z, \quad (1)$$

where  $S_i^x$  and  $S_i^z$  are components of spin- $\frac{1}{2}$  operators and the sums are performed over the internal and surface lattice points, respectively.  $E$  is an external electrical field. The quantity  $J_{ij}$  represents the strength of the interaction between spins at nearest neighbor sites  $i$  and  $j$ . The interaction of spins at the surface shell is denoted as  $J_{ij} = J_s$ , whereas

otherwise the interaction is  $J_b$ . In the same manner  $\Omega_b$  and  $\Omega_s$  represent transverse fields in the bulk and surface shell. It is important to mention that the exchange interaction  $J_{ij} \equiv J(r_i - r_j)$  depends on the distance between the spins, consequently the interaction strength is determined by the lattice parameters, the lattice symmetry and the number of next nearest neighbors. Starting from Eq. (1), compare [19], one finds immediately that the ordered phase is characterized by  $\langle S^x \rangle \neq 0$  and  $\langle S^z \rangle \neq 0$ . Therefore it is appropriate to introduce a new coordinate system by rotating the original one by the angle  $\theta$  in the  $x - z$  plane. The rotation angle  $\theta$  is determined by the requirement  $\langle S^{x'} \rangle = 0$  in the new coordinate system.

Since the lack of translational invariance the Green's function has to be investigated in the real space. The retarded Green's function is defined by

$$G_{lm}(t) = \ll S_l^+(t); S_m^-(0) \gg . \quad (2)$$

The operators  $S_l^+, S_m^-$  are the Pauli operators in the rotated system. The equation of motion of the Green's function in random phase approximation (RPA) reads

$$\begin{aligned} \omega G_{lm} &= 2\langle S_l^z \rangle \delta_{lm} + \left[ 2\Omega_l \sin \theta_l + \mu E \cos \theta_l + \sum_j J_{lj} \cos \theta_l \cos \theta_j \langle S_j^z \rangle \right. \\ &\quad \left. + \frac{1}{2} \sum_j J_{lj} \sin \theta_l \sin \theta_j (\langle S_l^+ S_j^- \rangle + \langle S_l^- S_j^+ \rangle) \right] G_{lm} \\ &\quad - \frac{1}{2} \sum_j J_{lj} [\sin \theta_l \sin \theta_j \langle S_l^z \rangle + 2 \cos \theta_j \cos \theta_l \langle S_l^+ S_j^- \rangle] G_{jm}. \end{aligned} \quad (3)$$

The poles of the Green's function give the transverse excitation energies. Within the applied RPA the transverse spin-wave energy is found as

$$\epsilon_n = 2\Omega_n \sin \theta_n + \frac{1}{N'} \sum_j J_{nj} \cos \theta_n \cos \theta_j \langle S_j^z \rangle + \mu E \cos \theta_n, \quad (4)$$

where  $N'$  is the number of sites in any of the shells. To complete the soft-mode energy  $\epsilon_n$  of the  $n$ -th shell, one needs the rotation angle  $\theta_n$ , which follows from the condition  $\langle S^{x'} \rangle = 0$ .

From here the angle is determined by the equation

$$-\Omega_n \cos \theta_n + \frac{1}{4} \sigma_n J_n \cos \theta_n \sin \theta_n + \frac{1}{2} \mu E \sin \theta_n = 0. \quad (5)$$

Using the standard procedure for Green's function we get the relative polarization of the  $n$ -th shell in the form

$$\sigma_n = \langle S_n^z \rangle = \frac{1}{2} \tanh \frac{\epsilon_n}{2T}. \quad (6)$$

### III. NUMERICAL RESULTS AND DISCUSSION

In this section we present the numerical results of the relevant quantities based on Eqs. (4, 5, 6). In particular, we analyze the behavior of spherical FE particles, which are depicted in Fig. 1. In case of BTO the bulk interaction parameter is  $J_b = 150$  K and the transverse field is  $\Omega_b = 10$  K. Due to the different numbers of next nearest neighbors on the surface the interaction strength  $J$  can take different values for the surface, denoted by  $J_s$ , and for the bulk, labeled as  $J_b$ , compare also [21]. Firstly, let us consider the hysteresis loop for different surface configurations represented by the interaction constant  $J_s$  at a fixed temperature  $T = 300$  K and fixed  $N$ . The results for a particle with  $N = 8$  shells are shown in Fig. 2.

One observes that the coercive field  $E_c$  is sensitive to variations of the interaction parameter  $J$ . If the coupling at the surface is smaller  $J_s = 50$  K as that in the bulk  $J_b = 150$  K (dashed line), the coercive field  $E_c$  and the remanent polarization  $\sigma_r$  are reduced in comparison to the case for  $J_s = J_b$  (solid line). With other words, the coercive field is lowered when the critical temperature of the system is decreased due to the smaller  $J_s$  value. In the opposite case  $J_s > J_b$  (dotted line) both, the coercive field  $E_c$  and the remanent polarization  $\sigma_r$  increase compared to  $J_s = J_b$ . Because of the enlarged value of  $J_s$  the phase transition temperature  $T_c$  of the small particle will be enhanced. The realization  $J_s < J_b$  may explain the decrease of the polarization  $\sigma$  and the phase transition temperature  $T_c$  observed in small BTO- [22] and PTO- particles [23]. The opposite case, namely a stronger coupling at the surface, is in agreement with observations made in small KDP- particles [24], where the polarization and the critical temperature increase compared to the bulk material.

In order to investigate the properties of BTO-type FE small particles we examine in the following the case  $J_s < J_b$  in more detail. The temperature dependence of the hysteresis loop for eight layers is shown in Fig. 3.

With increasing temperature the hysteresis loop is more compact and lower, the coercive field decreases and even for  $T \geq T_c$  the hysteresis loop vanishes (dashed line). Moreover, we have investigated the dependence of the remanent polarization  $\sigma_r$  and the coercive field  $E_c$  on the particle size  $N$ . The results are depicted in Fig. 4.

Both the field  $E_c$  (square) and the polarization  $\sigma_r$  (circle) increase with increasing  $N$ , which is in agreement with theoretically finding [18] and the experimental data from ultrathin FE

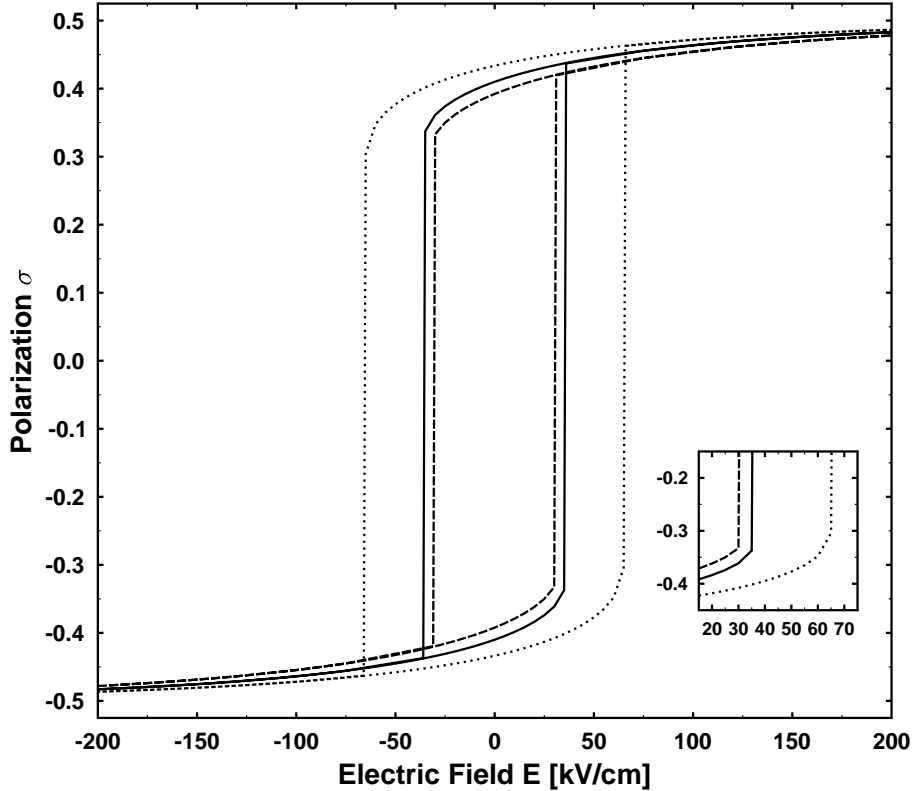


FIG. 2: Influence of the surface coupling strength  $J_s$  on the hysteresis at fixed temperature  $T = 300$  K,  $J_b = 150$  K and  $N = 8$ :  $J_s = 150$  K (solid curve),  $J_s = 350$  K  $> J_b$  (dotted curve),  $J_s = 50$  K  $< J_b$  (dashed curve); the insert offer the low field behavior .

BTO- films [25]. We found in our approach no rising coercive field with decreasing particle size as reported in [4, 5, 6, 7].

Because there are several experimental indications for a significant influence of doping effects on the hysteresis loop, now our model is modified in such a manner to include defects. Physically, such defects can be originated by localized vacancies or impurities, doping ions with smaller radii and larger distances in-between in comparison to the host material, see also [18]. Microscopically, the substitution of defects into the material leads to a change of the coupling parameter. Within our model let us assume that one or more of the shells are composed of defects. The interaction strength between neighbors  $J_d$  is altered and in general

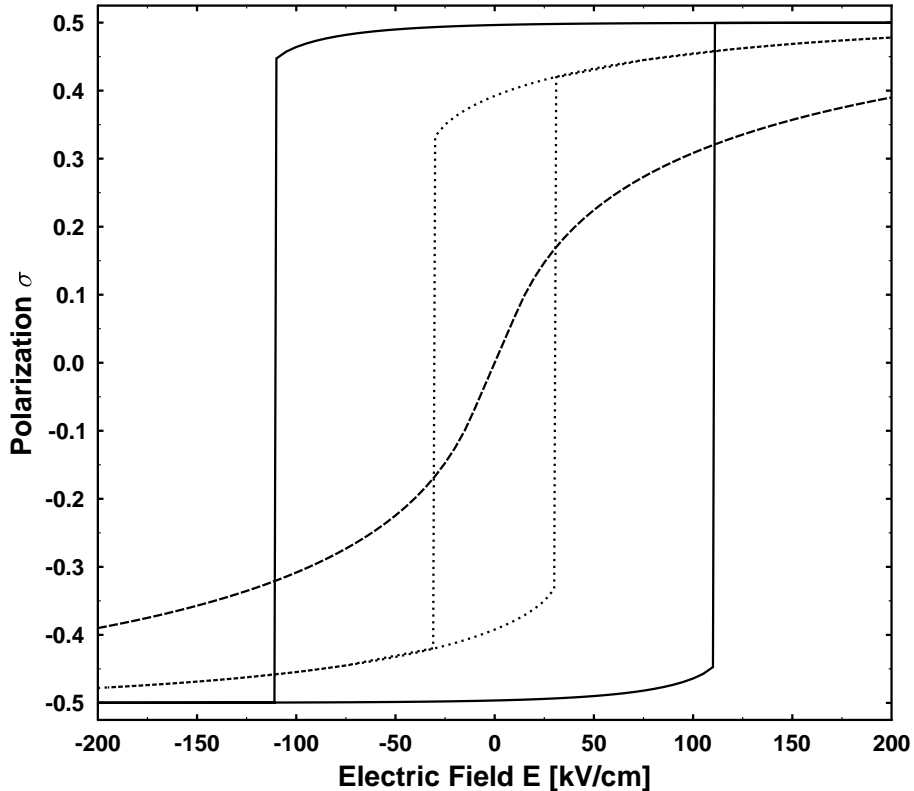


FIG. 3: Temperature dependence of the hysteresis with  $N = 8$ ,  $J_b = 150$  K,  $J_s = 50$  K:  $T = 100$  K (solid curve),  $T = 300$  K (dotted curve),  $T = 500$  K (dashed curve).

different from the surface value  $J_s$  as well as the bulk one  $J_b$ . Furthermore, the defect can be situated at different shells within the nanoparticle. In Fig. 5 we show the influence of defects with variable strength  $J_d$  on the hysteresis loop.

A single isolated defect layer offers only a weak influence on the hysteresis curve. Due to that we have studied the case that the first five layers of the nanoparticle are defect ones (compare also Fig. 1). Here the number of ferroelectric constituents is large enough to give a significant contribution to the polarization and consequently to the hysteresis loop. Apparently one observes a change of the shape of the hysteresis loop due to defects. In real materials one expect  $J_d < J_b$ . In that case the coercive field and the remanent polarization are reduced (dashed curve) compared to the case without defects  $J_d = J_b$  (solid curve). This

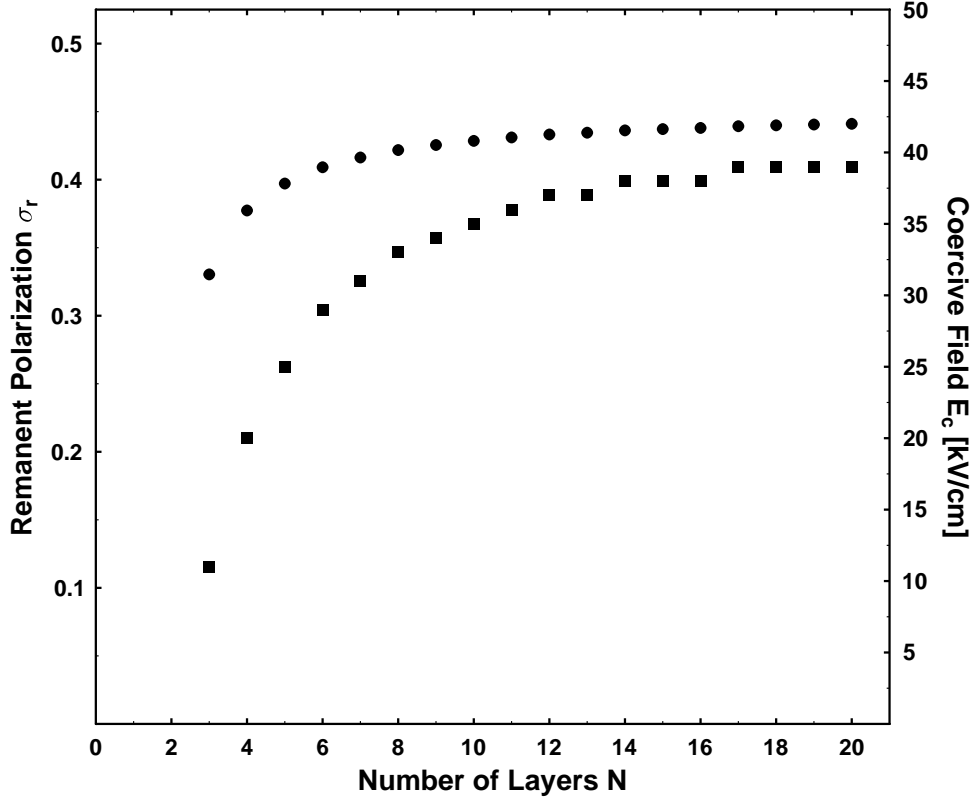


FIG. 4: Remanent polarization  $\sigma_r$  (circles) and coercive field  $E_c$  (squares) for different layers  $N$  at temperature  $T = 300$  K and couplings  $J_b = 150$  K,  $J_s = 50$  K.

may explain the experimentally observed decrease of  $T_c$ ,  $E_c$  and  $\sigma_r$  in small FE particles by the substitution of doping ions. The situation is for instance realized by substituting La in PTO [12] and PZT [13, 14] nanopowders. Although in the majority of real materials  $J_d$  should be smaller than  $J_b$ , we study also the opposite case  $J_d > J_b$ . The results are shown as the dotted curve in Fig. 5. The coercive field, the remanent polarization and the critical temperature are larger than those without defects (solid curve in (Fig. 5)). Such a situation, namely that the defect coupling is stronger than the bulk coupling will be realized, when the impurities have a larger radius compared to the constituent ions. The corresponding quantities are enhanced in comparison to the bulk value, which is clearly originated by an enhanced  $J_d$ -coupling, which is in accordance with the experimentally observed increase of

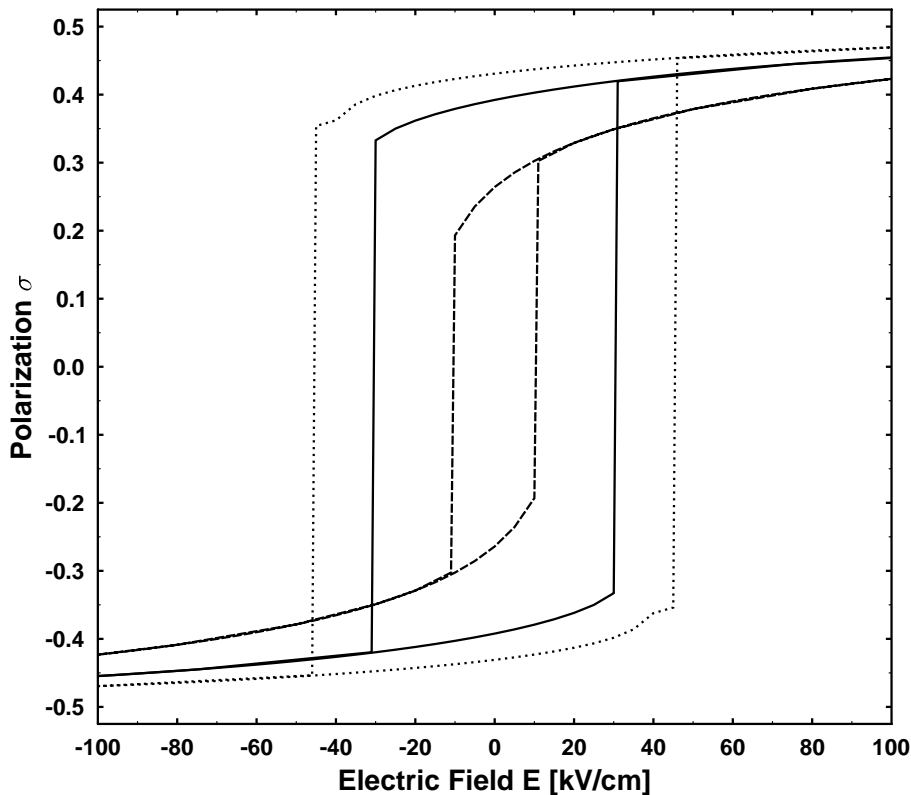


FIG. 5: Influence of defects on the hysteresis for  $T = 300$  K,  $J_b = 150$  K,  $J_s = 50$  K. From the total number of  $N = 8$  layers the first five layers are defect layers:  $J_d = J_b$  (solid curve);  $J_d = 400$  K (dotted curve);  $J_d = 25$  K (dashed curve).

$T_c$ ,  $E_c$  and  $\sigma_r$  by the substitution of doping ions, such as Bi in SBT [11] or by increasing the Ba contents in PLZT ceramics [15]. This behavior is in contrast to the case  $J_d < J_b$ . Let us stress that the variation of the interaction strength  $J$  can be also interpreted as the appearance of local stress, originated by the inclusion of different kinds of defects. The case  $J_d > J_b$  corresponds to a compressive stress, leading to an enhancement of  $E_c$ , which has been observed in thin PZT films [9]. The opposite case, i.e. tensile stress, yields to a decrease of  $E_c$ .

As visible in Figs. (4, 5) the coercive field and the remanent polarization of the FE particle are decreased or increased due to the different interaction strength within the defect shell.

Obviously the mentioned quantities should depend on the number of the inner defect shells, i. e. on the concentration of the defects. This dependence is shown in Fig. 6 for a particle with eight shells.

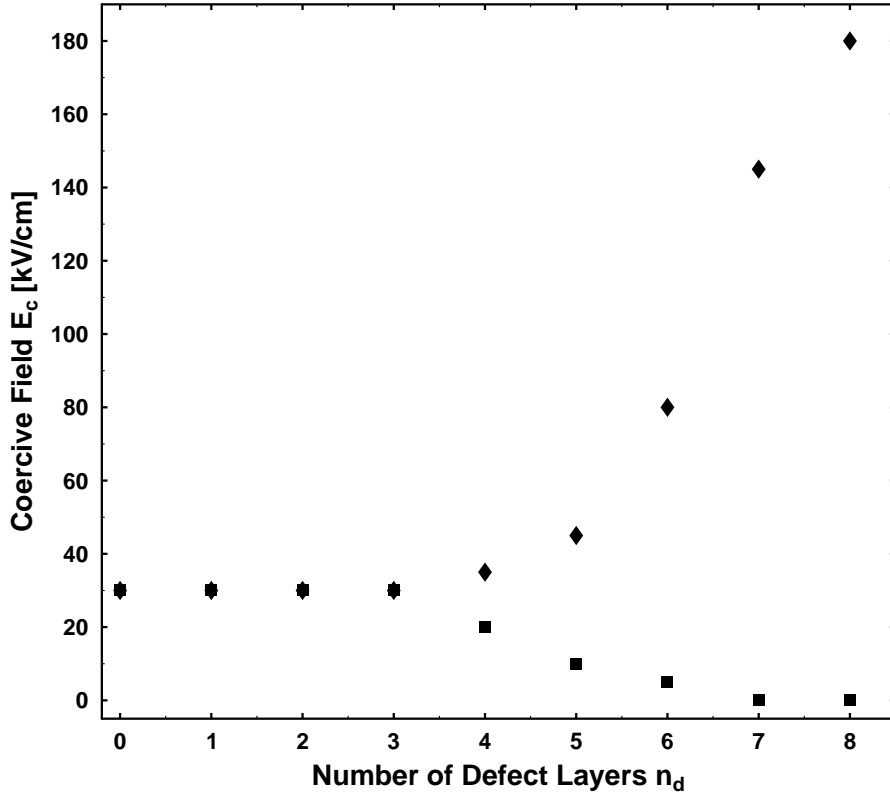


FIG. 6: Coercive field  $E_c$  in dependence on the number of defect layers  $n_d$  for  $N = 8$ ,  $J_b = 150$  K,  $J_s = 50$  K,  $T = 300$  K and different strength of  $J_d$ :  $J_d = 25$  K, i. e.  $J_b > J_d$  (squares) and  $J_d = 400$  K, i. e.  $J_d > J_b$  (diamonds) .

Notice that for instance  $n_d = 5$  means, that all layers until the fifth layers are defect layers, a situation which is precisely considered in Fig. 5. The squares in Fig. 6 demonstrates, that the coercive field strength  $E_c$  decreases with increasing number of defect shells, where we assume  $J_d = 25$  K, i.e.  $J_b > J_d$ . This result is in reasonable accordance to the experimental data given in [12, 13, 14]. A similar result is also obtained for the remanent polarization  $\sigma_r$ . An increase of the La content in PTO and PZT ceramics decreases the coercive field  $E_c$ .

The opposite behavior is offered as the diamonds in Fig. 6 with  $J_d = 400$  K, i.e.  $J_d > J_b$ . With increasing number of defect layers the coercive field  $E_c$  (respectively  $\sigma_r$ ) increases. This finding is in a quite good agreement with the experimental data offered by Noguchi et al. [11] and Ramam et al. [15].

Fig. 7 shows the dependence of the Curie temperature  $T_c$  on the number of defect layers  $n_d$  for a spherical particle.

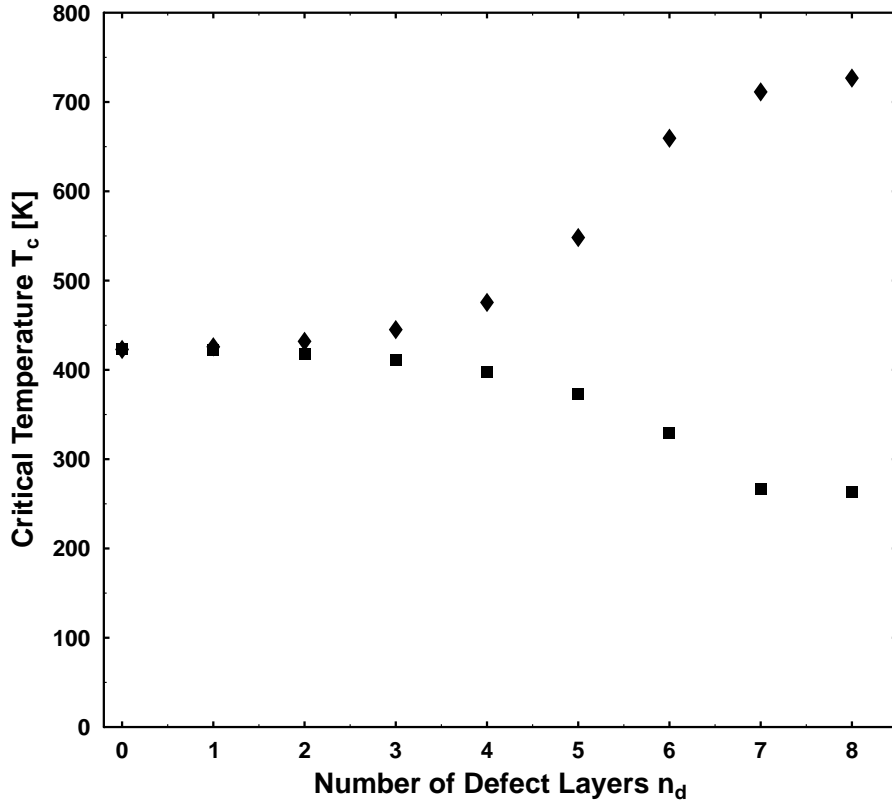


FIG. 7: Dependence of the critical temperature  $T_c$  on the number of defect layers  $n_d$  for  $N = 8$ ,  $J_b = 150$  K,  $J_s = 50$  K and different  $J_d$  couplings:  $J_d = 25$  K, i. e.  $J_b > J_d$  (squares) and  $J_d = 400$  K, i. e.  $J_b < J_d$  (diamonds) .

A defect coupling smaller than the bulk and surface couplings,  $J_d < J_b$  (squares), yields a decreasing critical temperature  $T_c$  with increasing number of defect shells, whereas in the opposite case (diamonds) the critical temperature increases with the number of defect

layers. The different behavior is controlled by the interaction strength. These results are in a qualitative agreement with the experimental data obtained by Noguchi et al. [26]. They have studied SBT films ( $T_c = 295^\circ\text{C}$ ) where the rare earth cations have been substituted by La, Ce, Pr, Nd and Sm as well as Bi at the A site (Sr site) with Sr vacancies. The La modification induces a soft behavior (lowering of  $E_c$  and  $P_r$ ), while a large amount of Nd and Sm substitution results in a very high  $E_c$  (hard). So the modified behavior is the result of defect engineering of both Sr and oxide vacancies. Likewise other bismuth layer-structured FE (BLSF) reveals that  $T_c$  is strongly influenced by the radius  $r_i$  of A-site cations. BLSF with smaller A-site cations ( $\text{Ca}^{2+}$ ) tends to a higher  $T_c$  ( $420^\circ\text{C}$ ). The inclusion of the same amount of  $\text{Ba}^{2+}$  (with larger radius) leads to a relaxation of FE distortions and results in a decrease of  $T_c$  to  $120^\circ\text{C}$ . The substitution of La with concentration  $x = 0.5$  gives rise to a marked decrease in  $T_c$  to  $180^\circ\text{C}$ , because the induced A-site vacancies weaken the coupling between neighboring  $\text{BO}_6$  octahedral [26, 27]. This result corresponds in our approach when the interaction parameter  $J_d$  is reduced, i. e.  $J_d < J_b$ . In La-modified  $\text{PbTiO}_3$  the transition temperature  $T_c$  decreases significantly, too, with an increase of the La content [28]. In Bi-SBT the critical temperature  $T_c$  increases strongly to  $405^\circ\text{C}$  ( $x=0.2$ ) [26]. The increase in  $T_c$  by Bi substitution tends to the opposite behavior as that observed in La-SBT. This is governed by the bonding characteristics with oxide ions. The influence of the orbital hybridization on  $T_c$  is very large, and Bi substitution results in a higher  $T_c$  [29]. This experimental observation is in a sufficient good agreement with our analytical finding when the interaction strength satisfies  $J_d > J_b$ .

#### IV. CONCLUSION

Because ferroelectricity at a nanoscale has emerged as a fertile ground for new physical phenomena we have analyzed in this paper FE nanoparticles based on a microscopic model. To this aim the Ising model in a transverse field is modified in such a manner that the effects of surfaces and defects are taken into account. Eventually, these properties are manifested within our model by introducing different microscopic coupling parameters for the constituents of the FE material. Due to the broken translational invariance the Green's function technique has to be formulated in real space. As the result of the equation of motion method for the Green's function we find the polarization of the nanoparticle depending on

an external electric field, the temperature, the defect position and concentration as well as the size of the particle. In particular, we are interested in the coercive field  $E_c$ , which is very sensitive to the interaction strength at the surface  $J_s$  and the presence of defects manifested by a microscopic coupling  $J_d$ . In case of a defect coupling strength that is lower than the bulk one,  $J_d < J_b$ , the coercive field, the remanent polarization  $\sigma_r$  and the Curie temperature  $T_c$  are reduced in comparison to the case without defects. This theoretical finding gives an explanation of the experimentally observations in FE small particles by substituting of doping ions, such as La in PTO [11], PZT [12,13] nanopowders. Contrary we get in the opposite case with  $J_d > J_b$  (for example when the impurities have a larger radius compared with the constituent ions), that the coercive field, the remanent polarization and the critical temperature are larger than the case without defects. This realization is in accordance with the experimental data showing an increase of  $T_c$ ,  $E_c$  and  $\sigma_r$  by the substitution of doping ions, such as Bi in SBT [10] or by increasing Ba contents in PLZT [14] ceramics. The dependence on the particle size is also discussed. Our results give strong indications that microscopic details of the interaction within the FE nanoparticles are essential for the macroscopic behavior of such a quantity as the hysteresis loop, whose shape seems to be important for practical applications of FE. In this paper we have demonstrated that one of the standard model for describing ferroelectric systems, namely the modified Ising model in a transverse field, is able to give explanation for experimental observations.

### **Acknowledgments**

One of us (J. M. W.) is grateful to the Cluster of Excellence in Halle for financial support. This work is further supported by the SFB 418. Further we acknowledge discussions with Marin Alexe and Dietrich Hesse, MPI Halle.

- 
- [1] M. Dawber, K. M. Rabe, and J. F. Scott, Rev. Mod. Phys. **77**, 1083 (2005).
- [2] J. T. Evans and R. Womack, IEEE J. Solid State Circuits. **23**, 1171 (1988).
- [3] O. Auciello, J. F. Scott and R. Ramesh, Phys. Today **51**, 22 (1998).
- [4] S. B. Ren, C. J. Lu, J. S. Liu, H. M. Shen and Y. N. Wang, Phys. Rev. B **54**, R14337 (1996).
- [5] N. A. Pertsev, J. Rodriguez Contreras, V. G. Kukhar, B. Hermanns, H. Kohlstedt and R. Waser, Appl. Phys. Lett. **83**, 3356 (2003).
- [6] S.-J. Jeong, M.-S. Ha and J.-H. Koh, Ferroel. **332**, 83 (2006).
- [7] V. Nagarajan, T. Zhao, J. Ouyang, R. Ramesh, W. Tian, X. Pan, D. S. Kim, C. B. Eom, H. Kohlstedt, and R. Waser, Appl. Phys. Lett. **84**, 5225 (2004).
- [8] J. S. Liu, S. R. Zhang, H. Z. Zeng, C. T. Yang and Y. Yuan, Phys. Rev. B **72**, 172101 (2005).
- [9] M. Lebedev and J. Akedo, Jpn. J. Appl. Phys. **41**, 6669 (2002).
- [10] S. Desu, J. Am. Ceram. Soc. **73**, 3391, 3398, 3407, 3416 (1990).
- [11] Y. Noguchi, M. Miyayama and T. Kudo, Phys. Rev. B **63**, 214102 (2001).
- [12] K. Iijima, R. Takayama, Y. Tomita and I. Ueda, J. Appl. Phys. **60**, 2914 (1986).
- [13] M. Tyunina, J. Levoska, A. Sternberg and S. Leppavuori, J. Appl. Phys. **84**, 6800 (1998).
- [14] M. Plonska, D. Czekaj and Z. Surowiak, Mater. Science **21**, 431 (2003).
- [15] K. Ramam and V. Miguel, Eur. Phys. J. Appl. Phys. **35**, 43 (2006).
- [16] N. Duan, J. E. ten Elshof, H. Verweij, G. Greuel and O. Dannapple, Appl. Phys. Lett. **77**, 3263 (2000).
- [17] V. C. Lo, J. Appl. Phys. **94**, 3353 (2003).
- [18] J. Wang and T.-Y. Zhang, Phys. Rev. B **73**, 144107 (2006).
- [19] R. Blinc and B. Žekš *Soft Modes in Ferroelectrics and Antiferroelectrics* (North-Holland, Amsterdam, 1974).
- [20] H. X. Cao and Z. Y. Li, J. Phys.: Condens. Matter **15**, 6301 (2003).
- [21] J. M. Wesselinowa, phys. stat. sol. (b) **223**, 737 (2001).
- [22] S. Schlag and H. F. Eicke, Solid State Commun. **91**, 883 (1994).
- [23] S. Chattopadhyay, P. Ayyub, V. R. Palkar and M. Multani, Phys. Rev. B **52**, 13177 (1995).
- [24] E. V. Colla, A. V. Fokin and Yu. A. Kumzerov, Solid State Commun. **103**, 127 (1997).
- [25] Y. S. Kim, D. H. Kim, J. D. Kim, Y. J. Chang, T. W. Noh, J. H. Kong, K. Char, Y. D. Park,

- S. D. Bu, J.-G. Yoon, and J.-S. Chung, Appl. Phys. Lett. **86**, 102907 (2005).
- [26] Y. Noguchi, M. Miyayama, K. Oikawa, T. Kamiyama, M. Osada and M. Kakihana, Jpn. J. Appl. Phys. **41**, 7062 (2002).
- [27] T. Sakai, T. Watanabe, H. Funakubo, K. Sarro and M. Osada, Jpn. J. Appl. Phys. **42**, 166 (2003).
- [28] T. Y. Kim and H. M. Jang, Appl. Phys. Lett. **77**, 3824 (2000).
- [29] R. R. Das, P. Bhattacharya, W. Perez and R. S. Katiyar, Jpn. J. Appl. Phys. **42**, 162 (2003).